Inorganic Chemistry

Article

pubs.acs.org/IC

Multinuclear Magnetic Resonance Investigation of Crystalline Alkali Molybdates

John E. C. Wren, Brandon J. Greer, Vladimir K. Michaelis,[†] Carolyn S. Higman, and Scott Kroeker*

Department of Chemistry, University of Manitoba, Winnipeg, Manitoba R3T 2N2, Canada

Supporting Information

ABSTRACT: A variety of crystalline alkali molybdate phases are characterized by ^{23}Na, ^{133}Cs, and ^{95}Mo magic-angle-spinning nuclear magnetic resonance (MAS NMR) to provide spectroscopic handles for studies of devitrification products in borosilicate nuclear waste glasses. The NMR parameters obtained from line-shape simulations are plotted as a function of various structural parameters to discern trends that may prove useful in the determination of unknown phases. These are applied to $Cs_3Na(MoO_4)_2$, the most common precipitate found in cesium- and molybdenum-bearing model nuclear waste glasses, the crystal structure of which has not yet been determined, to provide structural constraints that may guide the refinement of powder X-ray diffraction data.

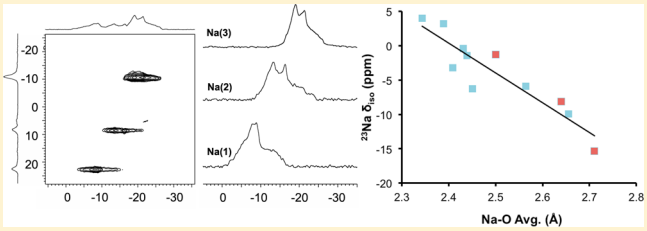

INTRODUCTION

Alkali molybdates form a diverse array of crystalline phases. Their rich variety is particularly relevant to the disposal of high-level radioactive waste, where these phases can form within highly durable waste glasses because of the limited solubility of molybdenum in borosilicate melts.[1−11] Studying these complex, mixed-phase precipitates in vitreous high-level waste storage materials is challenging by bulk analysis methods such as electron microprobe analysis or X-ray diffraction (XRD) because of the multiplicity of microcrystalline phases.[12,13] NMR spectroscopy offers the distinct advantage of probing each nucleus in the system individually, thereby reducing the number of phases observed in a single analysis to those containing the nucleus under observation.[1−3,4−15] The NMR parameters for a nucleus in a crystalline environment are typically sufficiently unique that the phases can be directly identified from their line shapes, provided their spectral signatures have been independently documented. By measurement of the NMR characteristics of pure alkali molybdates, their presence in complex multiphase materials can be readily determined from the "fingerprint" of their characteristic line shapes.[3−5,16]

The observed NMR parameters for a given solid phase are a direct measure of the local chemical environment around the observed nuclei. Therefore, through a study of the relationship between the NMR parameters and local structure, it may be possible to derive insights into the identities and structures of uncharacterized phases that may be encountered spectroscopically. For example, the average, variance, and/or range of metal−oxygen (M−O) bond lengths and angles for a given nuclide in a series of similar compounds have been shown to correlate with NMR parameters such as the isotropic chemical shift (δ_{iso}) and quadrupolar coupling constant (C_Q).[16−19]

The most common devitrification products found in model molybdenum-bearing nuclear waste glasses are Na_2MoO_4, $Na_2MoO_4{\cdot}2H_2O$, $Cs_3Na(MoO_4)_2$, and $CsNaMoO_4{\cdot}2H_2O$,[3,4] with the presence of hydrated phases indicating that water can penetrate these materials. The NMR parameters of $Cs_3Na(MoO_4)_2$ were previously characterized by magic-angle-spinning (MAS) NMR;[3,4] however, little is known about its crystal structure. $K_3Na(MoO_4)_2$[20] and $Rb_3Na(MoO_4)_2$[21] are included in this work because of their possible similarity with $Cs_3Na(MoO_4)_2$. $Na_6Mo_{10}O_{33}$, $Na_2Mo_2O_7$, and Cs_2MoO_4 have also been observed in various molybdenum-containing model waste glasses, the crystal structures of which have been reported. $Na_2Mo_2O_7$ was previously characterized by ^{23}Na MAS NMR,[1] but its ^{95}Mo NMR characteristics are unknown. This paper reports multinuclear magnetic resonance studies of various known and uncharacterized solid phases of interest to nuclear waste disposal, with the intent of determining the spectral signatures to aid in the quantification and identification of various molybdates that can precipitate from nuclear waste glasses.

EXPERIMENTAL SECTION

Solid-State Synthesis. Na_2MoO_4 (Aldrich, > 98%) was used without further purification. $Na_2MoO_4{\cdot}2H_2O$ was prepared by precipitation from a concentrated aqueous solution of Na_2MoO_4. Cs_2MoO_4 was prepared with a 1:1 molar ratio of MoO_3 and Cs_2CO_3. Reagents were intimately mixed using an agate mortar and pestle before heating in an alumina crucible in a box furnace. Decarbonation was achieved by heating at 420 °C for 12 h. The reaction mixture was subsequently heated to 725 °C and then slowly cooled to 375 °C over 12 h (30 °C/h). $CsNaMoO_4{\cdot}2H_2O$ was prepared by evaporation of a

Received: July 20, 2015
Published: October 5, 2015

© 2015 American Chemical Society

DOI: 10.1021/acs.inorgchem.5b01556
Inorg. Chem. 2015, 54, 9853−9861

Table 1. NMR Parameters for Alkali Molybdates

	^{23}Na MAS NMR			^{133}Cs MAS NMR		^{95}Mo MAS NMR		
compound	δ_{iso} (ppm)	C_Q (±0.05) (MHz)	η (±0.1)	δ_{iso} (±0.5) (ppm)	C_Q (±20) (kHz)	δ_{iso} (ppm)	C_Q (±0.05) (MHz)	η (±0.1)
Na_2MoO_4	3.2 ± 0.1	2.59	0.0			−32.9 ± 0.4	0.0 ± 0.1	n.d.
$Na_2MoO_4{\cdot}2H_2O$	−1.4 ± 0.5	0.88	0.2			8 ± 1	1.15	0.8
	4.1 ± 0.2	2.68	0.1					
$Na_2Mo_2O_7$	−5.9 ± 0.5	1.44	0.5			−25.2 ± 0.2	1.20	0.1
	−9.9 ± 0.5	2.57	0.2			−22.9 ± 0.3	1.26	0.9
$Na_6Mo_{10}O_{33}$	−8.2 ± 0.1	2.40	0.6 ± 0.2			n.d.	n.d.	n.d.
	−15.4 ± 0.1	2.02	0.6 ± 0.2			n.d.	n.d.	n.d.
	−1.3 ± 0.5	2.26	0.8 ± 0.2			n.d.	n.d.	n.d.
Cs_2MoO_4				51	170	−19.2 ± 0.5	0.48	1.0 ± 0.3
				−15	270			
$CsNaMoO_4{\cdot}2H_2O$	−0.4 ± 0.3	1.33	1 ± 0.2	−70	200	−31 ± 1	0.75	0.8 ± 0.2
$Cs_3Na(MoO_4)_2$	−11.8 ± 0.1	0.73	0.0	161	150	−15 ± 0.5	0.65	0.0
				−144	370			
$Rb_3Na(MoO_4)_2$	−6.2 ± 0.1	1.45	0.0			−16 ± 0.3	1.34	0.0
$K_3Na(MoO_4)_2$	−3.2 ± 0.2	1.4	0.0			−10 ± 1	1.8	0.8 ± 0.2

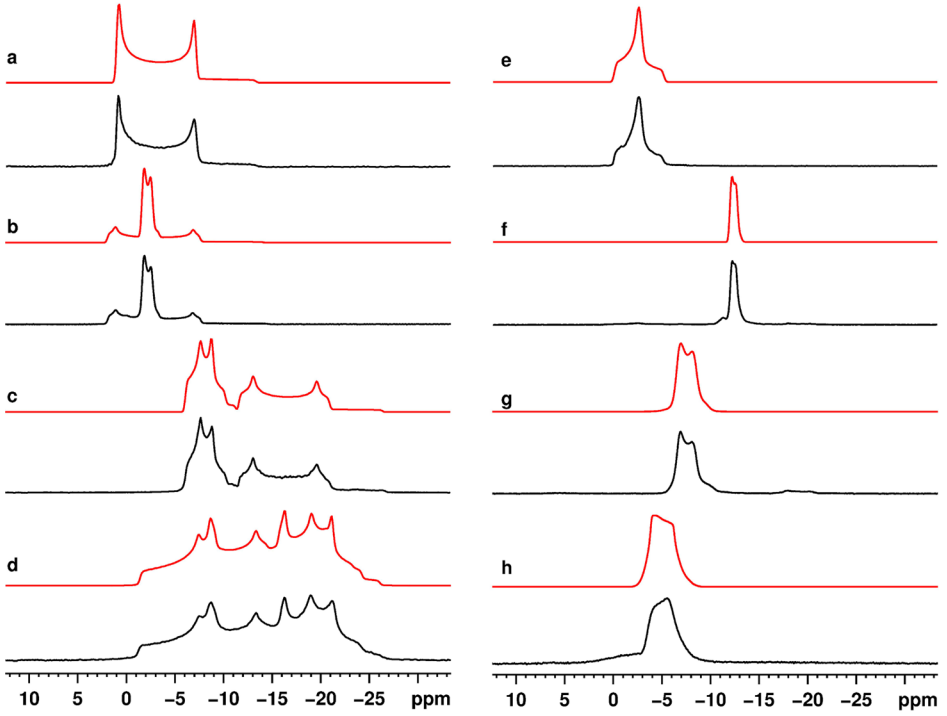

Figure 1. ^{23}Na MAS NMR of alkali molybdates at 14.1 T: experimental data (below, black) and simulated spectra (above, red) for (a) Na_2MoO_4, (b) $Na_2MoO_4{\cdot}2H_2O$, (c) $Na_2Mo_2O_7$, (d) $Na_6Mo_{10}O_{33}$, (e) $CsNaMoO_4{\cdot}2H_2O$, (f) $Cs_3Na(MoO_4)_2$, (g) $Rb_3Na(MoO_4)_2$, and (h) $K_3Na(MoO_4)_2$.

saturated 1:1 aqueous solution of sodium molybdate and cesium molybdate.

$Cs_3Na(MoO_4)_2$ is a novel compound synthesized by the high-temperature reaction of cesium carbonate, molybdenum trioxide, and sodium molybdate. The reagents were mixed and decarbonated at 420 °C for 12 h. Samples were then heated to 725 °C for 4 h, cooled to 550 °C (30 °C/h), held at this temperature for 1 h, then cooled to 375 °C for an additional 12 h, and finally cooled to 200 °C for 1 h. This heat-treatment process was repeated multiple times (2−4) for each sample to progressively increase the purity to above 98%, as determined by ^{133}Cs MAS NMR.

$Na_2Mo_2O_7$ was synthesized from a mixture of sodium carbonate and molybdenum trioxide and decarbonated at 550 °C for 12 h. The sample was then heated for 24 h at 600 °C. The sample purity was confirmed using ^{23}Na MAS NMR and powder XRD.[22−24]

$Na_6Mo_{10}O_{33}$ was synthesized[25] from a mixture of sodium carbonate and molybdenum trioxide. The mixture was decarbonated at 400 °C for 12 h and then heated to 530 °C for 48 h.

$K_3Na(MoO_4)_2$[20] and $Rb_3Na(MoO_4)_2$[21] were synthesized from a mixture of sodium carbonate, molybdenum trioxide, and either potassium or rubidium carbonate. The mixtures were decarbonated at 400 °C for 12 h and then heated to 600 °C for 48 h. All crystalline phases were verified using both NMR and powder XRD for crystalline purity (≥95%).

NMR Spectroscopy. MAS NMR spectra were collected on a Varian UNITY Inova 600 (B_0 = 14.1 T) spectrometer using single-pulse (Bloch decay) experiments with short tip angles of 13−23°. ^{133}Cs and ^{87}Rb MAS NMR spectra were collected on a 1.6 mm triple-resonance MAS probe with a spinning frequency (ν_{MAS}) of 30.000 ± 0.002 kHz, ν_{rf} = 71 and 100 kHz, respectively, and optimized recycle delays of up to 300 and 5 s, respectively, to ensure full relaxation (i.e.,

DOI: 10.1021/acs.inorgchem.5b01556
Inorg. Chem. 2015, 54, 9853−9861

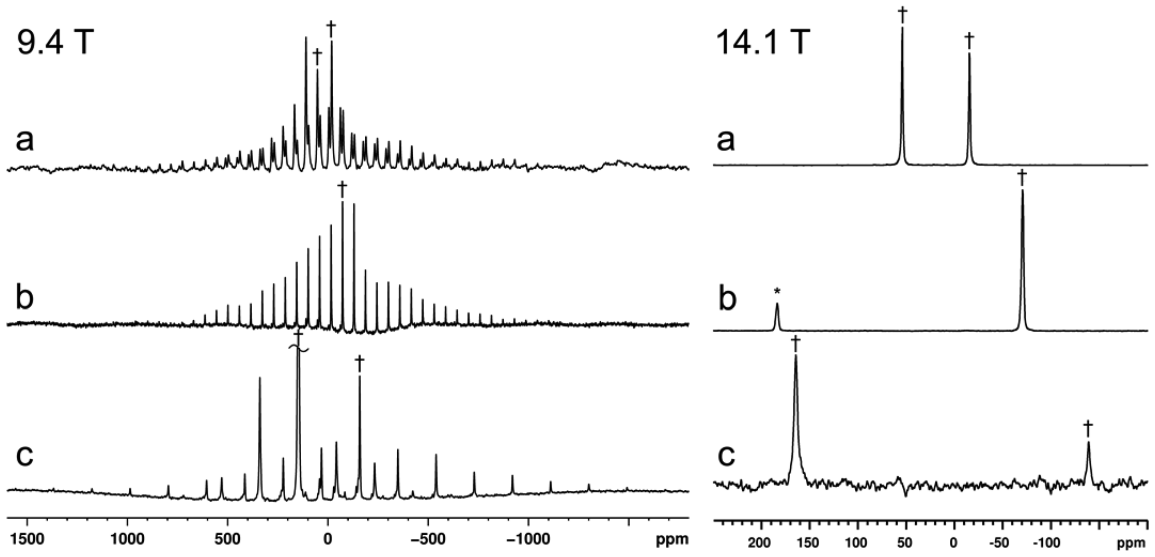

Figure 2. ^{133}Cs MAS NMR of alkali molybdates at 9.4 and 14.1 T: (a) Cs_2MoO_4 collected at ν_{MAS} = 3 kHz (9.4 T) and ν_{MAS} = 30 kHz (14.1 T); (b) $CsNaMoO_4{\cdot}2H_2O$ collected at ν_{MAS} = 3 and ν_{MAS} = 20 kHz; (c) $Cs_3Na(MoO_4)_2$ collected at ν_{MAS} = 10 and ν_{MAS} = 30 kHz. ^{133}Cs isotropic chemical shifts are indicated by a dagger.

$5T_1$). ^{23}Na MAS NMR spectra were acquired using a 3.2 mm double-resonance (DR) MAS probe, with ν_{MAS} = 20 kHz, ν_{rf} = 50 kHz, and recycle delays of up to 10 s. ^{23}Na multiple-quantum (3Q) MAS (*z*-filtered) NMR spectra were collected using a 1.6 mm triple-resonance MAS probe, with ν_{MAS} = 30.000 ± 0.002 kHz and ν_{rf} = 111 kHz, with both spectral dimensions rotor-synchronized. The spectrum was collected with 256 scans for each of the 60 t_1 increments using a recycle delay of 1 s. ^{95}Mo MAS NMR spectra were collected with a 5 mm DR MAS probe, with ν_{MAS} = 8.000 ± 0.005 kHz, ν_{rf} = 60 kHz, and recycle delays of 5−20 s.

^{23}Na and ^{87}Rb MAS NMR spectra for several samples were also collected at 9.4 T on a Bruker Avance III 400 spectrometer to confirm spectral-fitting parameters. Experiments were done using a 4 mm DR MAS probe with ν_{MAS} = 10 kHz, ν_{rf} = 53 kHz, and recycle delays of 2 s. Supplementary ^{95}Mo MAS NMR spectra were also collected at 9.4 T using a 4 mm single-channel low-γ MAS probe, with ν_{MAS} = 10 kHz, ν_{rf} = 75 kHz, recycle delays up to 30 s, and 1024−5120 coadded transients. All spectra were referenced using aqueous solutions: NaCl (1 M, 0 ppm, ^{23}Na), CsCl (0.5 M, 0 ppm, ^{133}Cs), RbCl (1 M, 0 ppm, ^{87}Rb), and Na_2MoO_4 (1 M, 0 ppm, $^{95/97}$Mo).

The NMR parameters were determined by fitting the spectra using simulation software *WSolids* and *DMfit*.[26,27] Fitting of all transitions for the slow-spinning ^{23}Na and ^{133}Cs MAS NMR data was accomplished using the QUASAR[28] solid-state NMR simulation package implemented within *DMfit 2011*. ^{87}Rb and ^{95}Mo MAS NMR data at 9.4 and 14.1 T were simultaneously simulated in *WSolids* using second-order quadrupolar line shapes.

Powder XRD. All crystalline phases were analyzed using a Bragg−Brentano powder X-ray diffractometer (PANalytical X'Pert Pro; diffractometer radius = 240 mm), employing Cu $K\alpha_{1,2}$ radiation (λ = 1.54098 and 1.544426 Å), and equipped with a diffracted beam nickel filter and an X'Celerator detector. Data sets were collected in the 2θ range 10−90° in 0.0083° steps. Samples were ground to a fine powder in an agate mortar and pestle and affixed to zero-background quartz sample holders using vacuum grease.

RESULTS AND DISCUSSION

NMR spectra are displayed in Figures 1−5 along with their corresponding spectral simulations; parameters are tabulated in Table 1. First, general observations about the different NMR nuclides are presented, followed by a discussion of each molybdate phase and finally a discussion of the relationships between the NMR parameters and various structural features.

^{23}Na MAS NMR. ^{23}Na NMR is a common structural technique largely because of its favorable spectroscopic characteristics. ^{23}Na (I = $^3/_2$) is the single naturally occurring isotope of sodium and features a relatively high magnetogyric ratio, γ, yielding a resonance frequency of 158.8 MHz at 14.1 T.[14] The chemical shift range of ^{23}Na in diamagnetic environments is narrow, whereas the quadrupole moment is moderate (10.4 fm^2), often resulting in broad and overlapped line shapes, making resolution of multiple sites challenging (see Figure 1). The isotropic chemical shifts, δ_{iso}(^{23}Na), for this series of molybdates range between 4.1 and −15.4 ppm, with C_Q values varying from 0.73 to 2.68 MHz and asymmetry parameters, η, from 0 to 1.

^{133}Cs MAS NMR. ^{133}Cs (I = $^7/_2$) has a moderate γ resulting in a resonance frequency of 78.69 MHz at 14.1 T and is the only naturally occurring isotope of cesium. The quadrupole moment of ^{133}Cs is very small (−0.34 fm^2), while the chemical shift range is large, often producing narrow, well-separated center bands in MAS NMR spectra. Because of the high polarizability of the cesium electron density, ^{133}Cs NMR powder patterns are often broadened by sizable chemical shielding anisotropy.[14]

In the molybdates studied here, δ_{iso}(^{133}Cs) values were found to range from −144 to 161 ppm, with C_Q values between 150 and 370 kHz (Figure 2). The breadth of the spinning-sideband manifold for ^{133}Cs spectra is likely due to the anisotropies of both the chemical shielding and quadrupolar interactions. The average breadth of the ^{133}Cs MAS NMR spinning-sideband manifold in the phases studied was approximately 2000 ppm (at 9.4 T). By iterative fitting of the spinning-sideband manifold, it became apparent that the total contribution to the breadth of the spinning-sideband manifold by anisotropic shielding could be no more than 200 ppm, i.e., <10% of the total breadth. Therefore, the spinning-sideband manifolds were accepted as reasonable approximations of the first-order quadrupolar couplings.

^{95}Mo MAS NMR. ^{95}Mo (I = $^5/_2$) is one of two NMR-active isotopes of molybdenum. ^{95}Mo NMR is typically chosen over ^{97}Mo NMR because of the smaller quadrupole moment (−2.2

DOI: 10.1021/acs.inorgchem.5b01556
Inorg. Chem. 2015, 54, 9853−9861

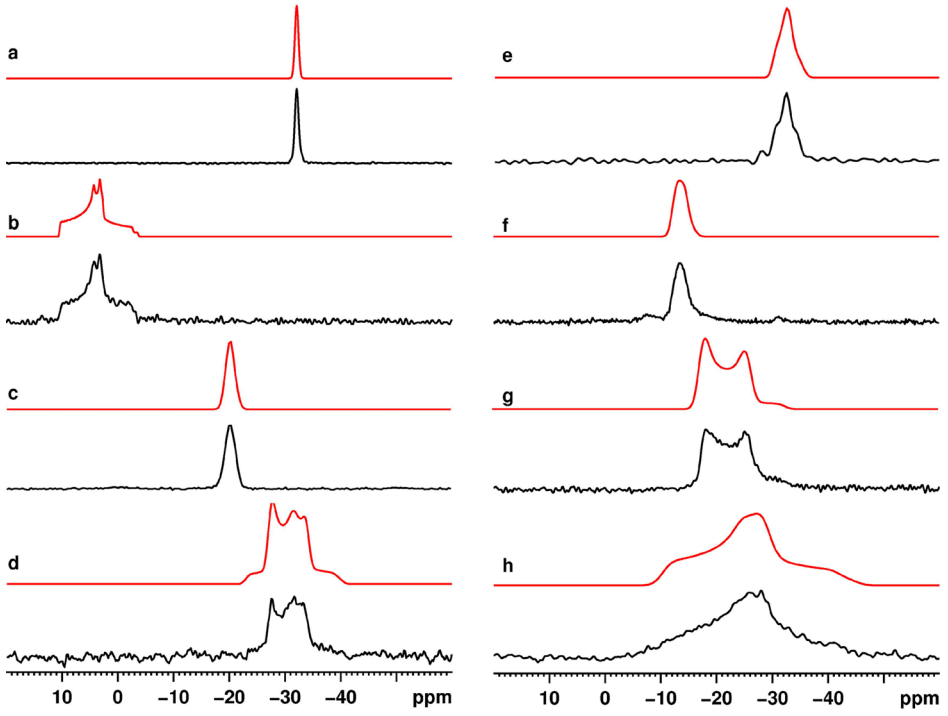

Figure 3. ^{95}Mo MAS NMR of alkali molybdates at 14.1 T: experimental (black, below) and spectral simulation (red, above) for (a) Na_2MoO_4, (b) $Na_2MoO_4{\cdot}2H_2O$, (c) Cs_2MoO_4, (d) $Na_2Mo_2O_7$, (e) $CsNaMoO_4{\cdot}2H_2O$, (f) $Cs_3Na(MoO_4)_2$, (g) $Rb_3Na(MoO_4)_2$, and (h) $K_3Na(MoO_4)_2$.

and 25.5 fm^2, respectively) and higher abundance (15.92 vs 9.46%). Because of the low magnetogyric ratios of both isotopes (39.3 and 40.14 MHz at 14.1 T, respectively), sensitivity is often a challenge. δ_{iso}(^{95}Mo) values for the studied samples were found to range between −32.9 and 8 ppm, C_Q values were found to lie between 0 and 1.34 MHz, and η values were in the range of 0−1 (Figure 3).

^{87}Rb MAS NMR. ^{87}Rb ($I = {}^3/_2$) is an isotope of rubidium with properties generally favorable for NMR studies, including a relatively high natural abundance of 27.8%, a moderate quadrupole moment (13.35 fm^2), and high resonance frequency (196.2 MHz at 14.1 T). ^{87}Rb MAS NMR spectra of $Rb_3Na(MoO_4)_2$ collected at multiple fields displayed distinct line shapes consistent with the two crystallographically inequivalent sites in $Rb_3Na(MoO_4)_2$.[21] The spectra were fit to two axially symmetric sites in a 2:1 integrated ratio with resonances at δ_{iso} = 44 and −80 ppm, having C_Q = 2.35 and 13.5 MHz, respectively (Figure S1).

NMR Parameters of Individual Molybdate Phases. *Na_2MoO_4.* Sodium molybdate exists at room temperature in a cubic unit cell and has been thoroughly studied by NMR.[29] The sodium ions occupy a single site located at a special position with $\bar{3}$ site symmetry. The observed ^{23}Na MAS NMR line shape has η = 0, consistent with the structure (Table 1 and Figure 1a), as previously reported.[29,30] The single molybdenum site in the structure is located at a position possessing T_d symmetry with the surrounding oxygen atoms, resulting in a narrow ^{95}Mo NMR peak with C_Q = 0 MHz (Figure 3a), in agreement with previous measurements.[30,31] To confirm that C_Q is actually zero and not simply smaller than our observed line width, we ran ^{97}Mo MAS NMR at 9.4 T, where the quadupole moment is more than an order of magnitude larger than that of ^{95}Mo (25.5 compared to −2.2 fm^2); there was no appreciable increase in the experimental line width (not shown).

$Na_2MoO_4{\cdot}2H_2O$. Sodium molybdate dihydrate has an orthorhombic unit cell,[32,33] with two crystallographically inequivalent sodium sites and one molybdenum site. One of the sodium cations coordinates to two water molecules and the oxygen atoms of three different molybdate (MoO_4^{2-}) units in a distorted square-pyramidal arrangement. The other sodium coordinates to four molybdate units and two water molecules in octahedral-type geometry. The six-coordinate site has been reported to possess a ^{23}Na line shape with C_Q = 0.88 MHz, while the five-coordinate site has C_Q = 2.68 MHz (Figure 1b).[30]

^{95}Mo MAS NMR of $Na_2MoO_4{\cdot}2H_2O$ produces a single resonance with a moderate C_Q of 1.15 MHz (Figure 3b). The central molybdenum ions coordinate to four oxygen atoms, with bond lengths varying from 1.75 to 1.78 Å. The asymmetrical environment formed by the Mo−O bonds gives rise to η = 0.8 and nonzero C_Q.

$Na_2Mo_2O_7$. Sodium dimolybdate has two crystallographically distinct sodium sites,[22] one with near-octahedral coordination and the other coordinated to eight oxygen atoms. The eight-coordinate site has Na−O bonds ranging from 1.86 to 2.79 Å, while the six-coordinate site has a smaller bond-length range of 1.92 to 2.45 Å. The ^{23}Na MAS NMR spectrum shows two distinct line shapes, with 1:1 integrated intensity ratio, consistent with the crystal structure (Figure 1c).

There are two molybdenum sites in the $Na_2Mo_2O_7$ crystal structure with a 1:1 occupancy (Figure 4). One is 4-fold-coordinated, with Mo−O bond lengths between 1.71 and 1.784 Å; the O−Mo−O angles vary from 106 to 111°. The other site is 6-fold-coordinated, with four short Mo−O bonds of either 1.68 or 1.90 Å and two longer bonds of 2.27 Å; the O−Mo−O angles range between 78.5 and 104.2°. The corresponding ^{95}Mo MAS NMR spectrum reveals overlapping line shapes at both fields used (Figures 3d and 4). Simultaneous fitting of the ^{95}Mo MAS NMR spectra was restricted to two sites in a 1:1 integrated ratio and produced plausible fits to the data at 14.1

DOI: 10.1021/acs.inorgchem.5b01556
Inorg. Chem. 2015, 54, 9853−9861

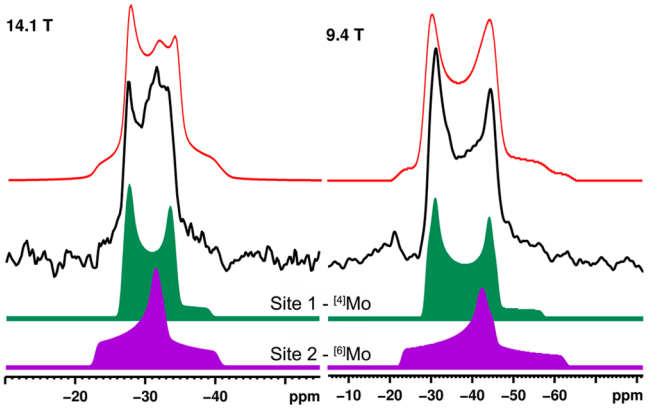

Figure 4. ^{95}Mo MAS NMR of $Na_2Mo_2O_7$ at 9.4 and 14.1 T. Site 1 (green, above): δ_{iso} = −25.2 ppm, η = 0.1, and C_Q = 1.2 MHz. Site 2 (purple, below): δ_{iso} = −22.9 ppm, η = 0.9, and C_Q = 1.26 MHz.

and 9.4 T with a single set of NMR parameters, δ_{iso}, C_Q, and η (Figure 4). The similarity of the chemical shift and quadrupolar coupling constants for these two sites does not discriminate conveniently between these two different polyhedra. However, the difference in the quadrupolar asymmetry allows the low-η line shape to be assigned to the 4-coordinate site because its nearness to tetrahedral symmetry, or at least C_3 rotational symmetry, would bias the quadrupolar tensor toward axial symmetry. The significant deviation from colinearity along the axial O−Mo−O bonds of the 6-coordinate site, meanwhile, is more likely to produce a quadrupolar asymmetry parameter nearer to 1.

$Na_6Mo_{10}O_{33}$. $Na_6Mo_{10}O_{33}$ is a complex molybdate phase with three crystallographically unique sodium sites and five unique molybdenum sites.[25] One of the three sodium sites is 6-coordinate in a pseudooctahedral environment and the other two are 7-coordinate, each with bond lengths ranging from 2.26 to 3.09 Å. The ^{23}Na MAS NMR of $Na_6Mo_{10}O_{33}$ (Figure 1d) appears to consist of several overlapped line shapes. ^{23}Na MQMAS NMR acquired on this sample to separate the overlapping line shapes (Figure 5a) clearly reveals the three inequivalent ^{23}Na sites. Parameters determined for the three sites observed in the MQMAS NMR (Figure 5b) were applied to the one-dimensional Bloch decay spectrum to produce a unique three-site fit of the data with the expected 1:1:1 integrated ratio (Figure 5c). These signals were assigned to their crystallographic sites using the established relationship between δ_{iso} and the average Na−O bond length (see below, Figure 6a).[14,18,34]

The five molybdenum ions each coordinate with six oxygen atoms, but the local site symmetry is highly distorted from an ideal octahedron, with O−Mo−O bond angles as small as 43.917° and as wide as 128.815°.[25] The multiplicity of sites combined with presumably large quadrupolar coupling constants to stymie attempts to record the ^{95}Mo MAS NMR spectrum of $Na_6Mo_{10}O_{33}$. The resulting signal was broad and featureless and could not be separated into its constituent components (not shown).

Cs_2MoO_4. The two cesium sites in the orthorhombic unit cell of cesium molybdate are present in a 1:1 ratio.[35,36] One cesium cation is asymmetrically coordinated to 11 oxygen atoms at Cs−O bond distances between 2.95 and 4.08 Å. A second site has a more regular 9-fold-coordinated geometry, with Cs−O distances ranging from 3.05 to 3.60 Å. The ^{133}Cs MAS NMR spectrum of Cs_2MoO_4 has central peaks at +51 and −15 ppm with integrated intensities of approximately 3:2 (Figure 2a). The C_Q value was estimated by fitting the spinning-sideband manifold. The sidebands for the higher-frequency site (51 ppm) were simulated with a C_Q value of approximately 170 kHz, whereas the site at −15 ppm was simulated with a C_Q value of 270 kHz. This difference in C_Q is responsible for the apparent discrepancy between the integrated relative intensities of the NMR peaks (3:2) and the crystal structure (1:1).[37] On the basis of these NMR parameters, the peak at −15 ppm may be assigned to the 11-coordinate site because (a) the larger C_Q is consistent with the higher degree of polyhedral distortion in this site and (b) the chemical shifts of larger coordination spheres are typically associated with more negative chemical shifts.[34,38,39]

^{95}Mo MAS NMR shows a single resonance corresponding to the single 4-coordinate site in the crystal structure. The Mo−O bond lengths vary narrowly between 1.77 and 1.78 Å, and the bond angles are likewise similar, ranging from 108.5° to 110.1°. This subtle geometrical variation is consistent with the relatively small C_Q (480 kHz) measured from the central transition line shape; however, the absence of T_d symmetry is reflected in the asymmetry parameter of 1 (Figure 3c).

$CsNaMoO_4{\cdot}2H_2O$. The orthorhombic unit cell of $CsNaMoO_4{\cdot}2H_2O$ has sodium ions in near-octahedral symmetry,[40] coordinated to the oxygen atoms of two MoO_4^{2-} units in axial positions, with four water molecules coordinated equatorially. This environment is consistent with the moderate C_Q (1.33 MHz) observed in the ^{23}Na MAS NMR spectrum (Figure 1e and Table 1). The low point-group symmetry at the sodium site gives rise to the high quadrupolar asymmetry parameter of 1.

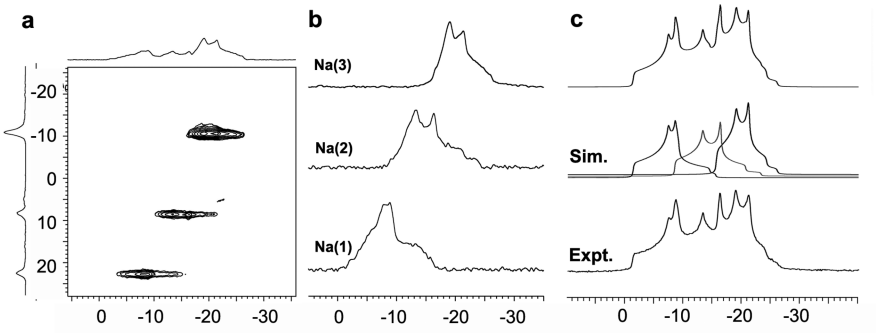

Figure 5. ^{23}Na NMR of $Na_6Mo_{10}O_{33}$: (a) 2D MQMAS; (b) slices of the three sites resolved in the isotropic dimension; (c) 1D MAS spectrum with overall simulation and subspectra.

DOI: 10.1021/acs.inorgchem.5b01556
Inorg. Chem. 2015, 54, 9853−9861

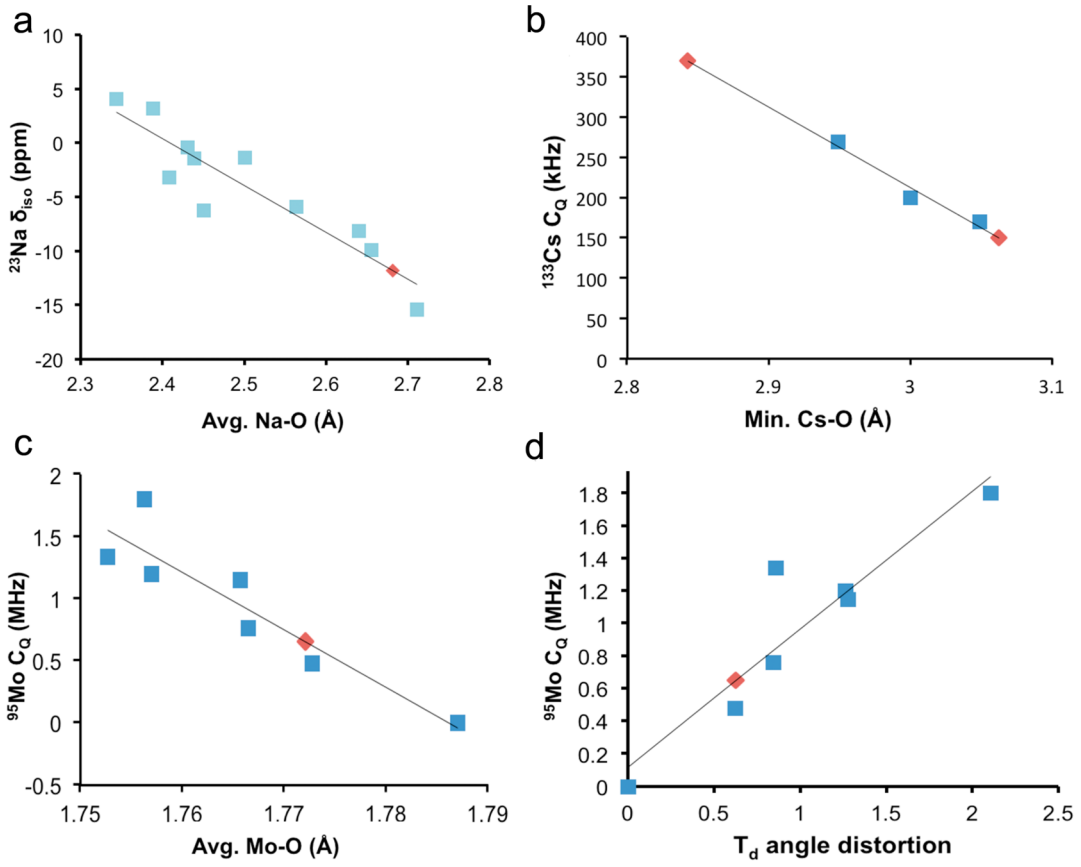

Figure 6. Correlation plots between NMR parameters measured for alkali molybdates and various structural metrics: (a) $\delta_{iso}(^{23}Na)$ as a function of the average Na−O bond length (R^2 = 0.84), (b) $C_Q(^{133}Cs)$ as a function of the minimum Cs−O bond length (R^2 = 0.95), (c) $C_Q(^{95}Mo)$ as a function of the average Mo−O bond length (R^2 = 0.85), (d) $C_Q(^{95}Mo)$ as a function of the tetrahedral bond-angle distortion factor, σ^2 (R^2 = 0.86). Red diamonds represent interpolations for $Cs_3Na(MoO_4)_2$, the crystal structure of which is unknown.

The cesium ions are 12-fold-coordinated with contacts to various molybdate and water oxygen atoms, with Cs−O bond distances between 3.00 and 4.06 Å. The corresponding ^{133}Cs NMR resonance is only a few ppm broad under MAS, with no evidence of second-order quadrupolar effects. Accordingly, C_Q was estimated to be 200 kHz by simulating the spinning-sideband manifold with all NMR transitions (see Figure 2b).

The molybdenum site has near-tetrahedral symmetry, with O−Mo−O bond angles of either 110 or 108°. Three of the Mo−O bond lengths are 1.76 Å, with a fourth longer bond of 1.78 Å. The distorted tetrahedral geometry is consistent with the nonzero asymmetry parameter (η = 0.75) observed in the ^{95}Mo MAS NMR (Figure 3e).

$Rb_3Na(MoO_4)_2$. This compound was included as a reference to illuminate the unknown structure of $Cs_3Na(MoO_4)_2$. $Rb_3Na(MoO_4)_2$ crystallizes in a hexagonal unit cell[21] with two distinct rubidium sites in an occupancy ratio of 1:2. Rb(1) is positioned at the corners of the hexagonal unit cell and coordinates to a total of 12 oxygen atoms in D_{3h} symmetry. Six of the nearest oxygen atoms are organized in a distorted octahedral arrangement with bond lengths of 3.04 Å. The other six oxygen atoms lie in the plane perpendicular to the C_3 rotation axis and have much longer Rb−O distances of 3.54 Å. Rb(2) has two equivalent positions, coordinating to 10 oxygen atoms in nearly C_{3v} point-group symmetry; Rb(2)−O interatomic distances range from 2.65 to 3.27 Å.

^{87}Rb MAS NMR spectra at two fields were fit to two line shapes with η = 0, consistent with the axial symmetry at both rubidium sites (Figure S1). The peaks can be assigned based on their relative integrated intensities, with Rb(1) assigned to the line shape at δ_{iso} = −80 ppm with the larger C_Q (13.5 MHz) and lower intensity, while Rb(2) is represented by the narrower (C_Q = 2.3 MHz), more intense signal located at +44 ppm. The high coordination number and longer Rb−O bond lengths are consistent with the highly shielded position of Rb(1).[34]

^{23}Na MAS NMR of $Rb_3Na(MoO_4)_2$ reveals a single line shape, consistent with the crystal structure. The spectrum was fit with a C_Q of 1.45 ± 0.05 MHz and η = 0 (Figure 1g). The single sodium site coordinates with six oxygen sites in D_{3d} symmetry, in agreement with the measured value of η = 0.

^{95}Mo MAS NMR of $Rb_3Na(MoO_4)_2$ reveals a single line shape, as expected from the crystal structure. The spectrum was fit with C_Q of 1.34 ± 0.02 MHz and η = 0 (Figure 3g). The molybdenum sits at a site of formally C_s point-group symmetry but is within experimental error of C_{3v}, explaining the axial symmetry measured in the electric-field-gradient (EFG) tensor. Correlations of the ^{95}Mo NMR parameters with structural trends (see below) reveal that the Mo−O bond lengths and angles of $Rb_3Na(MoO_4)_2$ fall slightly outside the expected trend, suggesting either that the rubidium cation has a subtle influence on the molybdenum electronic environment or that the crystal structure requires further refinement.

$K_3Na(MoO_4)_2$. This phase was indexed in a monoclinic space group ($C2/c$),[20] quite unlike the higher-symmetry space group found for $Rb_3Na(MoO_4)_2$. The potassium sites are in a 2:1 ratio, with potassium ions located in irregular polyhedra,

DOI: 10.1021/acs.inorgchem.5b01556
Inorg. Chem. 2015, 54, 9853−9861

coordinating to 10−12 oxygen atoms. The sodium site sits in a position of relatively high point-group symmetry (D_{2h}). Molybdenum is present in a relatively distorted tetrahedron, with low point-group symmetry (C_1), leading to the largest ^{95}Mo C_Q (1.8 MHz) measured for this series of compounds and a high degree of quadrupolar asymmetry (η = 0.8; Figure 3h).

$Cs_3Na(MoO_4)_2$. The crystal structure of $Cs_3Na(MoO_4)_2$ has not been reported in the literature; however, the trends documented below provide some insight into the probable structure of this phase.

Two ^{133}Cs MAS NMR peaks were found in a 2:1 ratio with significantly different values of δ_{iso} and C_Q: the higher-frequency and higher-intensity site (161 ppm) possesses a C_Q value of approximately 150 kHz (Figure 3c), whereas C_Q of the lower-frequency peak (−144 ppm) is more than twice that (370 kHz). The integrated intensities of these two sites, the very large chemical shift differences, and the relative magnitudes of the observed C_Q values are consistent with the ^{87}Rb MAS NMR parameters of $Rb_3Na(MoO_4)_2$, suggesting a high degree of similarity between these structures, which share the same stoichiometry.

The ^{23}Na MAS NMR spectrum of $Cs_3Na(MoO_4)_2$ has a single resonance with a relatively small quadrupole coupling of 0.73 MHz and η = 0 (Figure 1f and Table 1). The ^{23}Na line shape is broadened, with poorly resolved inflections compared to the other molybdates. This appears to be consistent with the $Rb_3Na(MoO_4)_2$ structure, which has a single sodium site with local D_{3d} point-group symmetry; any rotation axis greater than C_2 produces an axially symmetric EFG.[16]

The ^{95}Mo MAS NMR spectrum of $Cs_3Na(MoO_4)_2$ has a single resonance, which was fit to a moderate C_Q of 650 kHz and η = 0 (Figure 3f).

Correlations between the NMR Parameters and Structure in Alkali Molybdates. *^{23}Na NMR.* Sodium cations form ionic bonds with oxygen over a range of 1.8−2.9 Å in this set of compounds. Their coordination numbers range from 5 to 8, with most sodium cations found in distorted octahedral coordination. A variety of relationships were explored between the ^{23}Na NMR parameters (δ_{iso}, C_Q, and η) and various structural parameters (O−Na−O bond angles, Na−O bond lengths, and distortion parameters) (Figure S2). The only relationship showing reasonable correlation (R^2 = 0.84) is between the ^{23}Na isotropic chemical shifts and average Na−O bond lengths (Figure 6a). This trend has also been found for several other NMR nuclei and is used to estimate the bond lengths and coordination numbers in glasses.[34,38,41] The decrease in δ_{iso} with increasing interatomic distance is attributed to the decreasing influence of the oxygen atom on the ^{23}Na shielding.

^{133}Cs NMR. Defining reliable correlations for ^{133}Cs in cesium-bearing molybdates is complicated by the ambiguity in determining the Cs−O bonds that contribute to the polyhedron. Some cesium sites could be considered to be coordinated to as many as 17 oxygen atoms, with interatomic distances ranging from 2.95 to 4.86 Å (Gagne, O. C.; Hawthorne, F. C. University of Manitoba, personal communication). In the present analysis, we have limited meaningful interactions to r(Cs−O) < 4.1 Å, leading to coordination numbers no larger than 12. The most convincing correlations are with the shortest Cs−O contact, which circumnavigates the need to define the outer limit of the coordination sphere. Figure 6b shows C_Q(^{133}Cs) as a function of the minimum Cs−O interatomic distance for the three ^{133}Cs NMR data points for which reliable structural data are available, yielding an R^2 value of 0.95. Despite the paucity of data points in the plot, this dependency may be attributed to the likelihood that the largest component of the chemical shielding (δ_{33}) and the quadrupolar coupling tensors (V_{ZZ}) are approximately oriented along the shortest internuclear distance. These tensor components have a strong influence on the observed δ_{iso} and C_Q, and therefore their magnitude changes with the shortest interatomic distance. This approach has the additional advantage of being insensitive to long contacts and should not be influenced by uncertainties in the coordination sphere cutoff. Unlike the ^{23}Na trend reported above, the average Cs−O distance was found to be weakly correlated, at best, with any NMR measurable, including δ_{iso} (Figure S3). This may be due to the generally weaker Cs−O interactions and associated uncertainty in assigning the effective coordination environment.

^{95}Mo NMR. Molybdenum(VI) is a high-field-strength cation, with the implication that most of its oxides consist of isolated tetrahedral MoO_4^{2-} units. With the exceptions of $Na_2Mo_2O_7$, which has molybdenum sites arranged in chains of octahedral and tetrahedral moieties, and $Na_6Mo_{10}O_{33}$, where the five molybdate units form distorted 5- and 6-coordinate polyhedra, all molybdates studied here are built around the MoO_4^{2-} anion. Interestingly, the bond length and angle parameters for the octahedral site of $Na_2Mo_2O_7$ consistently fall well outside of the correlations tested, while the ^{95}Mo MAS NMR spectrum of $Na_6Mo_{10}O_{33}$ is too complicated to be included in the analysis.

C_Q appears to be the ^{95}Mo NMR observable most sensitive to the local geometry, showing convincing correlations with average Mo−O bond length, tetrahedral distortion parameter, and maximum and minimum O−Mo−O bond angles (Figures 6c,d and S4b), whereas δ_{iso} and η do not appear to be sensitive to these structural parameters ($R^2 \leq 0.49$; Figure S4).

The correlations between the molybdenum polyhedral structure and C_Q may be attributed to its dependence on a single EFG tensor element (V_{ZZ}) in nearly tetrahedral geometry. Pure tetrahedral geometry has cubic symmetry and hence no gradient in the electric field, leading to C_Q = 0. Any deviation of a molybdenum site from pure T_d symmetry, therefore, results in measurable changes in C_Q, as witnessed in these systems. Accordingly, a correlation (R^2 = 0.86) is found between the ^{95}Mo C_Q and the tetrahedral bond-distortion parameter, σ^2 (Figure 6d):

$$\sigma^2 = \frac{1}{6}\sum_{i}^{6}(\angle\mathrm{O{-}Mo{-}O}_i - 109.47°)^2$$

This parameter is an established metric representing the variance between the O−Mo−O bond angles away from the ideal tetrahedral bond angle (109.47°).[42] A related metric for analyzing the degree of bond angle distortion for pseudotetrahedral molybdenum is simply the absolute range of bond angles, Δ_{O-Mo-O}, calculated as the difference between the largest and smallest O−Mo−O angles. Δ_{O-Mo-O} shows a promising correlation with the quadrupolar coupling constant, R^2 = 0.73 (Figure S4). The relationship between C_Q and Δ_{O-Mo-O} qualitatively reflects the close connection between the EFG and local symmetry.

The Mo−O bond lengths prove to be less clearly correlated with NMR parameters, probably because of their small variation (1.74−1.87 Å). The average bond length gives a negative correlation (R^2 = 0.85) with C_Q(^{95}Mo) (Figure 6c).

DOI: 10.1021/acs.inorgchem.5b01556
Inorg. Chem. 2015, 54, 9853−9861

Structural Inferences about $Cs_3Na(MoO_4)_2$. Despite significant efforts, a single crystal of $Cs_3Na(MoO_4)_2$ large enough for X-ray crystallography could not be obtained nor could a sufficiently pure powder sample be synthesized for a reliable Rietveld refinement. While work in this area is ongoing, the relationships between NMR measurables and various geometrical elements defined here for alkali molybdates may be used to propose some structural parameters. For example, the average Na−O bond length in $Cs_3Na(MoO_4)_2$ may be predicted to be 2.68 Å based on the reasonably convincing correlation between the average Na−O bond length and $\delta_{iso}(^{23}Na)$ (Figure 6a). Despite having only three data points to define the trends, the ^{133}Cs NMR parameters δ_{iso} and C_Q show suggestive correlations with the minimum bond Cs−O bond lengths, indicating that these values for the two sites in $Cs_3Na(MoO_4)_2$ may be 2.8 and 3.1 Å (Figure 6b). Similarly, plots of $\delta_{iso}(^{133}Cs)$ and $C_Q(^{133}Cs)$ as a function of the average Cs−O bond lengths lead to values of 2.9 and 3.2 Å, respectively, for the lower-coordinate site and 3.7 and 3.8 Å for the higher-coordinate site (Figure S3). The most convincing correlations involving ^{95}Mo NMR parameters and the geometry of the MoO_4^{2-} anion indicate an average Mo−O bond length of 1.77 Å, with O−Mo−O bond angles between 110 and 108° (Figures 6c and S4) based on C_Q; $\delta_{iso}(^{95}Mo)$ predicts these angles to be 110 and 107° (Figure S4c). Although all of these structural parameters are subject to significant uncertainty because of the size of the data sets, variations in the composition, and other possible effects, they provide starting points for structural investigations and may be used as constraints on future refinements of high-quality XRD or neutron diffraction data.

CONCLUSION

NMR spectroscopic signatures have been obtained for a variety of crystalline alkali molybdates found as devitrification products in borosilicate nuclear waste glasses. In addition to documentation of individual phases for future studies, some general trends were established that may assist in assigning and identifying unknown phases that can precipitate from complex waste glass compositions. ^{23}Na MAS NMR may be used as a highly informative technique but is prone to significant spectral overlap when multiple sites are present. The large ^{23}Na quadrupole couplings and small chemical shift range common to molybdates can make them challenging to study, necessitating careful peak deconvolution and/or multiple-quantum techniques. Nevertheless, the chemical shift of ^{23}Na in molybdates shows a potentially valuable correlation with the average Na−O interatomic distance, providing a useful indicator for estimating the size of Na^+ sites in novel molybdate phases. ^{133}Cs MAS NMR of these molybdates is notable for its narrow center bands and wide chemical shift dispersion, permitting convenient identification of multiple phases. The geometrical asymmetry in Cs^+ sites decreases the chemical shift and increases the ^{133}Cs C_Q value. Despite the technical challenges involved in ^{95}Mo NMR, the measured parameters display persuasive correlations with the local structure in the phases studied. The ^{95}Mo C_Q value is particularly sensitive to the Mo−O bond lengths and asymmetry at the Mo^{6+} site in these molybdates. These relationships were used to place structural constraints on various geometrical parameters in $Cs_3Na(MoO_4)_2$, the crystal structure of which has not been reported. This work provides the basis for more effective NMR studies of phase separation in glasses related to radioactive waste disposal,[2−5,7,13] especially in situ experiments designed to better understand the mechanisms by which molybdates crystallize from high-temperature oxide melts.[11]

ASSOCIATED CONTENT

Supporting Information

The Supporting Information is available free of charge on the ACS Publications website at DOI: 10.1021/acs.inorgchem.5b01556.

^{87}Rb MAS NMR spectra of $Rb_3Na(MoO_4)_2$ and selected ^{23}Na, ^{133}Cs, and ^{95}Mo NMR correlation plots provided as Figures S1−S4 (PDF)

AUTHOR INFORMATION

Corresponding Author

*E-mail: scott.kroeker@umanitoba.ca. Tel: 204-474-9335.

Present Address

†V.K.M.: Department of Chemistry and Francis Bitter Magnet Laboratory, Massachusetts Institute of Technology, Cambridge, MA 02138.

Notes

The authors declare no competing financial interest.

ACKNOWLEDGMENTS

Dr. Mario Bieringer and Joey Lussier (University of Manitoba) are thanked for helpful discussions and access to their X-ray diffractometer. The Natural Sciences and Engineering Research Council (NSERC) of Canada, the Canada Foundation for Innovation, and the Province of Manitoba are acknowledged for generous support of this research. V.K.M. is grateful to NSERC for a postgraduate scholarship.

REFERENCES

(1) Greer, B. J. M.Sc. Thesis, University of Manitoba, Winnipeg, Manitoba, Canada, 2012.

(2) Kroeker, S. In *Encyclopedia of Magnetic Resonance*; Harris, R. K., Wasylishen, R. E., Eds.; John Wiley: Chichester, U.K., 2011.

(3) Kroeker, S.; Farnan, I.; Schuller, S.; Advocat, T. In *Scientific Basis for Nuclear Waste Management XXXII*; Rebak, R. B., Hyatt, N. C., Pickett, D. A., Eds.; Materials Research Society: Warrendale, PA, 2009; Vol. *1124*.

(4) Kroeker, S.; Higman, C. S.; Michaelis, V. K.; Svenda, N. B.; Schuller, S. In *Scientific Basis for Nuclear Waste Management XXXIV*; Smith, K. L., Kroeker, S., Uberuaga, B., Whittle, K. R., Eds.; Materials Research Society: Warrendale, PA, 2010; Vol. *1265*.

(5) Kroeker, S.; Schuller, S.; Greer, B.; Wren, J. E. C. *J. Am. Ceram. Soc.* **2015**, submitted for publication.

(6) Magnin, M.; Schuller, S.; Mercier, C.; Trebosc, J.; Caurant, D.; Majerus, O.; Angeli, F.; Charpentier, T. *J. Am. Ceram. Soc.* **2011**, *94*, 4274.

(7) Martineau, C.; Michaelis, V. K.; Schuller, S.; Kroeker, S. *Chem. Mater.* **2010**, *22*, 4896.

(8) Schuller, S.; Pinet, O.; Penelon, B. *J. Am. Ceram. Soc.* **2011**, *94*, 447.

(9) Caurant, D.; Majerus, O.; Fadel, E.; Quintas, A.; Gervais, C.; Lenoir, M.; Pinet, O. *J. Am. Ceram. Soc.* **2007**, *90*, 774.

(10) Rose, P. B.; Woodward, D. I.; Ojovan, M. I.; Hyatt, N. C.; Lee, W. E. *J. Non-Cryst. Solids* **2011**, *357*, 2989.

(11) Wren, J. E. C. Ph.D. Thesis, University of Manitoba, Winnipeg, Manitoba, Canada, 2014.

(12) Short, R. J.; Hand, R. J.; Hyatt, N. C.; Möbus, G. *J. Nucl. Mater.* **2005**, *340*, 179.

(13) Greer, B.; Kroeker, S. *Phys. Chem. Chem. Phys.* **2012**, *14*, 7375.

DOI: 10.1021/acs.inorgchem.5b01556
Inorg. Chem. 2015, 54, 9853−9861

(14) Mackenzie, K. J. D.; Smith, M. E. *Multinuclear Solid-State NMR of Inorganic Materials*, 1st ed.; Elsevier Science Ltd.: Kidlington, Oxford, U.K., 2002; Vol. *6*.
(15) Caurant, D.; Majerus, O.; Fadel, E.; Quintas, A.; Gervais, C.; Charpentier, T.; Neuville, D. *J. Nucl. Mater.* **2010**, *396*, 94.
(16) Wasylishen, R. E.; Ashbrook, S. E.; Wimperis, S. *NMR of Quadrupolar Nuclei in Solid Materials*; John Wiley & Sons: New York, 2012; Vol. *7*.
(17) Fayon, F.; Farnan, I.; Bessada, C.; Coutures, J.; Massiot, D.; Coutures, J. P. *J. Am. Chem. Soc.* **1997**, *119*, 6837.
(18) Stebbins, J. F. *Solid State Ionics* **1998**, *112*, 137.
(19) Michaelis, V. K.; Kroeker, S. *J. Phys. Chem. C* **2010**, *114*, 21736.
(20) Fabry, J.; Petricek, V.; Vanek, P.; Cisarova, I. *Acta Crystallogr., Sect. B: Struct. Sci.* **1997**, *53*, 596.
(21) Bai, C.; Lei, C.; Pan, S.; Wang, Y.; Yang, Z.; Han, S.; Yu, H.; Yang, Y.; Zhang, F. *Solid State Sci.* **2014**, *33*, 32.
(22) Seleborg, M. *Acta Chem. Scand.* **1967**, *21*, 499.
(23) Singh Mudher, K.; Keskar, M.; Krishnan, K.; Venugopal, V. *J. Alloys Compd.* **2005**, *396*, 275.
(24) Hoermann, F. *Z. Anorg. Allg. Chem.* **1929**, *177*, 145.
(25) Gatehouse, B.; Jenkins, C.; Miskin, B. *J. Solid State Chem.* **1983**, *46*, 269.
(26) Eichele, K. *WSolids1*, version 1.20.20; Universität Tübingen: Tübingen, Germany, 2013.
(27) Massiot, D.; Fayon, F.; Capron, M.; King, I.; Le Calve, S.; Alonso, B.; Durand, J. O.; Bujoli, B.; Gan, Z.; Hoatson, G. *Magn. Reson. Chem.* **2002**, *40*, 70.
(28) Amoureux, J.-P.; Fernandéz, C. *QUASAR-Solid State NMR Simulation for Quadrupole Nuclei*; University of Lille, Lille, France, 2005.
(29) Bottelberghs, P.; Van Buren, F. *J. Solid State Chem.* **1975**, *13*, 182.
(30) Skibsted, J.; Jakobsen, H. J. *Solid State Nucl. Magn. Reson.* **1994**, *3*, 29.
(31) d'Espinose de Lacaillerie, J.-B.; Barberon, F.; Romanenko, K. V.; Lapina, O. B.; Le Pollès, L.; Gautier, R.; Gan, Z. *J. Phys. Chem. B* **2005**, *109*, 14033.
(32) Matsumoto, K.; Kobayashi, A.; Sasaki, Y. *Bull. Chem. Soc. Jpn.* **1975**, *48*, 1009.
(33) Capitelli, F.; Selim, M. D.; Mukherjea, K. K. *Asian J. Chem.* **2006**, *18*, 2856.
(34) Michaelis, V. K.; Aguiar, P. M.; Kroeker, S. *J. Non-Cryst. Solids* **2007**, *353*, 2582.
(35) Gonschorek, W.; Hahn, T. *Z. Kristallogr. - Crystalline Materials* **1973**, *138*, 167.
(36) Kools, F. X. N. M.; Koster, A. S.; Rieck, G. D. *Acta Crystallogr., Sect. B: Struct. Crystallogr. Cryst. Chem.* **1970**, *26*, 1974.
(37) Massiot, D.; Bessada, C.; Coutures, J. P.; Taulelle, F. *J. Magn. Reson.* **1990**, *90*, 231.
(38) Xue, X.; Stebbins, J. F. *Phys. Chem. Miner.* **1993**, *20*, 297.
(39) Xu, Z.; Stebbins, J. F. *Solid State Nucl. Magn. Reson.* **1995**, *5*, 103.
(40) Makitova, D.; Tkachev, V.; Chekhlov, A. *Russ. J. Coord. Chem.* **2003**, *29*, 163.
(41) Koller, H.; Engelhardt, G.; Kentgens, A. P.; Sauer, J. *J. Phys. Chem.* **1994**, *98*, 1544.
(42) Locherer, K. R.; Swainson, I. P.; Salje, E. K. H. *J. Phys.: Condens. Matter* **1999**, *11*, 4143.

DOI: 10.1021/acs.inorgchem.5b01556
Inorg. Chem. 2015, 54, 9853−9861